

Density matrix renormalization group study of dimerization of the Pariser-Parr-Pople model of polyacetylene.

G. L. Bendazzoli, S. Evangelisti
 Dipartimento di Chimica Fisica e Inorganica, Università di Bologna
 viale Risorgimento 4, 40136 Bologna - Italy

G. Fano, F. Ortolani and L. Ziosi
 Dipartimento di Fisica, Università di Bologna
 Via Imerio 46, 40126 Bologna - Italy
 fano@bologna.infn.it
 (August 26, 2021)

We apply the DMRG method to the Pariser-Parr-Pople Hamiltonian and investigate the onset of dimerization. We deduce the parameters of the hopping term and the contribution of the bonds from *ab initio* calculations on ethylene. Denoting by R_{ij} the C-C distances, we perform a variational optimization of the dimerization $\langle (R_{i,i+1} - R_{i-1,i})^2 \rangle$ and of the average bond length R_0 for chains up to $N = 50$ sites. The critical value of N at which the transition occurs is found to be between $N = 14$ and $N = 18$ for the present model. The asymptotic values for large N for R_0 and $\langle (R_{i,i+1} - R_{i-1,i})^2 \rangle$ are given by $1.408(3)\text{Å}$ and $0.036(0)\text{Å}$.

I. INTRODUCTION

The quantum chemical treatment of large polymeric systems is extremely demanding from the computational point of view. When the electron correlation is taken into account, traditional correlated quantum chemical methods grow too rapidly with the number of electrons (n^5 or worse) to be considered as practical tools to study large systems. Density Functional Theory (DFT) is a powerful tool to cope with this kind of problems, and a number of efficient codes are available nowadays. However, the local density approximation (even with gradient corrections) can only treat the local part of the electron-electron correlations (within an atom or bond) and does not treat the interatomic correlations with sufficient accuracy. Moreover, no information on the wave function of the system is provided by this method. In this paper we focus our attention on a different method, i.e. the Density Matrix Renormalization Group (DMRG) formalism, proposed by White¹. This approach in principle can also be developed to an efficient tool to compute correlated energies and wave functions of the ground or excited states of large systems. DMRG is an approximation method that uses a density matrix to identify the most relevant states of a full configuration interaction (FCI) expansion. The localized orbital set is divided into two adjacent parts called "system" and "environment". The DMRG method allows one to determine in a precise mathematical way the most probable states of the "system" in the presence of the "environment". These states are retained, and the others are dropped. The calculation starts with two small fragments, whose size is increased in the course of the calculation, until the whole system reaches the wanted dimension. We refer the reader to Refs. [1,2] and [3] for a detailed description of the method.

DMRG has been applied to a wide class of systems, including strongly-correlated electrons, antiferromagnetic

Heisenberg chains⁴, phonons^{5,6}, defined on one and two dimensional lattices⁷. Originally DMRG was designed to treat nearest-neighbor interactions in one dimension, and in these conditions the method is very efficient in reducing the computational effort.

The Pariser-Parr-Pople (PPP) Hamiltonian of conjugated polyenes⁸ was recently studied with DMRG^{9,3}. In Ref. [9] the dimerized problem was considered with a symmetrized version of DMRG¹⁰ that allows the selection of excited states of given symmetry. In Ref. [3] the ground state at constant bond length was examined, and the results were in full agreement with FCI calculations, in all cases where these latter were available^{11,12}. The PPP Hamiltonian has a long history since in spite of its simplicity it provides at least a qualitative explanation of the essential physics of polyacetylene^{13,14}. We decided to consider the dimerization of the Pariser-Parr-Pople model of conjugated polyenes. Systematic studies of the bond alternation in conjugated polyenes were carried out by Paldus and coworkers^{15,16}. These authors used various kinds of approximations (self-consistent field, alternant molecular orbitals, coupled cluster, valence bond) since the FCI treatment ceases to be applicable before the onset of the bond alternation. It seems therefore interesting to compare those results with DMRG calculations on the same Hamiltonian. Recently a Density Functional (DFT) computation on large annulenes has been performed¹⁷, so a comparison of our DMRG results obtained with a model Hamiltonian with a realistic all-electron calculation can give useful information on the properties of the PPP model. DMRG has already been applied to the study of dimerization^{18,21} of polyacetylene chains using various model Hamiltonians. In Ref. [18], the authors considered a generalization of the Hubbard model to describe the valence electrons and approximated the contributions by a sum of pair interactions. Their generalization of the Hubbard model consisted of

allowing for a distance-dependent hopping term, while the Coulomb on-site repulsion was taken to be independent of the distance between C-C atoms. They determined the parameters of the model from accurate *ab initio* CI calculations on the ground state and the first excited state of the ethylene molecule, available as a function of the C-C distance²². The dimerization and the average bond-length R were determined minimizing the energy.

The aim of this paper is to exploit the same method for the determination of the parameters as a function of the C-C distance, and to improve the treatment of the correlation by substituting the crude Hubbard approximation with the more accurate PPP treatment of the Coulomb repulsion. For this purpose a generalization of the PPP Hamiltonian is used where both the hopping integral and the potential depend on the geometry of the system. In this way, the values of the average C-C distance and of the bond-alternation can be determined by a variational calculation as a function of N . Furthermore different geometries can be easily considered, which was not the case for the Hubbard model.

II. DEFINITION OF THE MODEL

To describe dimerization in trans-polyacetylene chains we introduce the following distance dependent Hamiltonian:

$$H = H_0 + H_1 \quad (2.1)$$

The contribution is approximated by a sum over all bonds and depends only on the bond lengths:

$$H_1 = \sum_{\langle ij \rangle} E(R_{ij}) \quad (2.2)$$

(R_{ij} is the distance between two carbon atoms located at sites i and j and $\langle ij \rangle$ denotes summation restricted to nearest neighbors). The contribution is represented by the Pariser-Parr-Pople Hamiltonian, with distance dependent hopping:

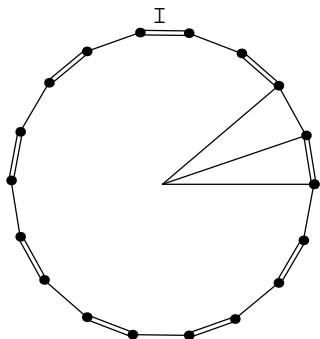


FIG. 1. Structure I: all C atoms are on a ring.

$$H = \sum_{\langle ij \rangle} t_{ij} \hat{E}_{ij} + \frac{1}{2} \sum_{ij=0}^N t_{ij} (\hat{n}_i - 1) (\hat{n}_j - 1) \quad (2.3)$$

Here \hat{E}_{ij} are the generators of the unitary group summed over spin, and $\hat{n}_i = \hat{E}_{ii}$ is the occupation number of the site i ; t_{ij} , t_{ij} are parameters of the model. For the Coulomb repulsion we use the Mataga-Nishimoto prescription²³:

$$t_{ij} = \frac{1}{\epsilon_0^{1/2} + R_{ij}} \quad (\text{a. u.}) \quad (2.4)$$

where $\epsilon_0 = 10.84$ eV.

Following Ref. [18] we determine t_{ij} and H_1 by imposing that the singlet-triplet splitting calculated *ab initio* for the ethylene molecule is correctly reproduced. In Ref. [22] the singlet-triplet splitting and the sign a energy are given as polynomial expansions in the bond length:

$$g(R) = ({}^3E(R) - {}^1E(R)) = 2 \sum_{l=1}^5 a_l R^l \quad (2.5)$$

$$E(R) = \sum_{l=1}^5 a_l^0 R^l \quad (2.6)$$

(the coefficients a_1 and a_1^0 are given in Table III of Ref. [22]). To make contact with our Hamiltonian, we calculate the singlet-triplet splitting applying H_1 to the ethylene molecule. Let us denote the singlet and triplet lowest energy states as:

$$|{}^3s\rangle = \cos \frac{\bar{p} \bar{a} b i - \bar{p} \bar{a} b i}{\sqrt{2}} + \sin \frac{\bar{p} \bar{a} i + \bar{p} b i}{\sqrt{2}} \quad (2.7)$$

$$|{}^1s\rangle = \frac{\bar{p} \bar{a} b i + \bar{p} b i}{\sqrt{2}} \quad (2.8)$$

It is easy to show that ${}^3E = \langle {}^3s | H_1 | {}^3s \rangle = 0$ while the singlet energy is:

$${}^1E(R) = \langle {}^1s | H_1 | {}^1s \rangle = \frac{1}{2} [(\epsilon_0 - t_{1;2}(R))^2 + 16 t_{1;2}^2(R)] \quad (2.9)$$

where the t_{ij} are given in Eq. 2.4. This is to be equated to $2g(R)$ and solved to give the dependence of $t_{1;2}$ on the bond length:

$$t_{1;2}(R) = \frac{s}{g^2(R) + \frac{g(R)}{2} \frac{\epsilon_0^2 R}{1 + \epsilon_0 R}} \quad (2.10)$$

Using the Mataga-Nishimoto prescription for ϵ_0 , we obtain for example $\epsilon_0 = 2.936160$ eV when $R = 1.40$ Å.

II

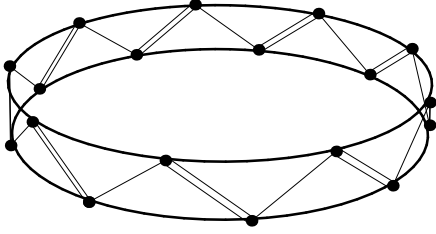


FIG. 2. Structure II: all C atoms are on the surface of a cylinder, all bond angles are equal to 120° .

III. DMRG ALGORITHM AND BOUNDARY CONDITIONS

We are now ready to implement the DMRG procedure. At every stage the actual sites are decomposed into sub-blocks forming a "superblock" $A \otimes B$ (where \otimes denotes a single site). Initially A and B are single site blocks. In order to enlarge the blocks, the reduced density matrix of the "system" $A \otimes B$ is computed and its most representative states are retained to define a basis of the new block $A \otimes B$ for the next iteration. The blocks B are obtained from the blocks A through reflection.

Once the total size of the whole system is reached, the algorithm may be continued with an asymmetric decomposition $A \otimes B$ with A and B different from one another. We can increase A and decrease B and vice-versa, optimizing the states that describe the blocks. This part is called finite-size algorithm, opposed to the first part called in finite-size algorithm (see Refs. [13] for details).

Generally in DMRG calculations open boundary conditions are imposed because the decay of the density matrix eigenvalues is faster with respect to the case of periodic boundary conditions and therefore the convergence is more accurate. We have tested that this difference is still present even with a long ranged potential, as in our case. When the system is finite the properties of the system depend on the choice of the boundary conditions. We put our system on a ring (structure I shown in Fig. 1), since it is a common experience in finite-size calculations that the absence of boundaries ensures a nice (smooth) scaling of the energy with the system size. Let us denote by r_c the circle radius. We want to consider only closed

shell system s , since the behaviour of the closed shell energies with respect to N is quite smooth²⁴ (the same is also true for low lying excited states that have an open shell structure and the same symmetry).

To obtain a closed shell state, we use periodic boundary conditions (PBC) for $N = 4 + 2$ and antiperiodic boundary conditions (ABC) for $N = 4$ (denoting by c_i the annihilation operator corresponding to the site i , ABC amount to put $c_N = -c_0$). In fact the allowed pseudomomenta are:

$$k_n = \begin{cases} \frac{2\pi n}{N} & \text{PBC} \\ \frac{2\pi n}{N} + \frac{\pi}{N} & \text{ABC} \end{cases} \quad n < \frac{N}{2} \quad (3.1)$$

We denote by θ_{01} and θ_{12} the two angles seen from the center corresponding to the double and single bond respectively, by θ_{ij} the angle between sites i and j , by R_0 the average bond-distance and by θ the dimerization:

$$R_0 = \frac{R_{i,j+1} + R_{i-1,j}}{2} \quad (3.2)$$

From the equations:

$$R_0 \cos \theta_{01} = 2r_c \sin \frac{\theta_{01}}{2} \quad (3.3)$$

$$R_0 \cos \theta_{12} = 2r_c \sin \frac{\theta_{12}}{2} \quad (3.4)$$

$$\frac{\theta_{01} + \theta_{12}}{2} = \frac{2\pi}{N} \quad (3.5)$$

it is easy to deduce that the circumference radius is given by:

$$r_c = \frac{R_0 \sqrt{\cos^2(\frac{\theta_{01}}{2}) + \sin^2(\frac{\theta_{12}}{2})}}{\sin(\frac{2\pi}{N})} \quad (3.6)$$

III

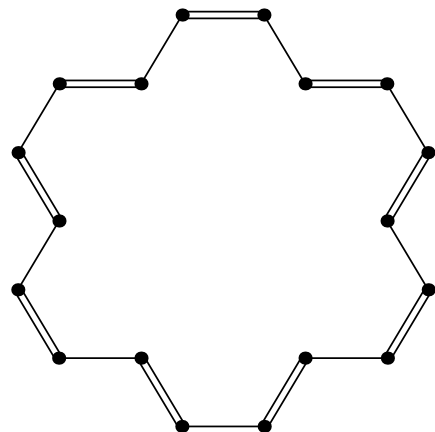


FIG. 3. Structure III: annulene D_{3h} geometry, proper of $6(2n + 1)$ system s , here shown for $N = 18$. All bond angles are equal to 120° .

Other geometries are also possible. In particular, one can fix the bond angles to 120° . This value is close to the experimental bond angle of the sp^2 hybridized carbon in linear polyenes. Two different geometrical arrangements of the atoms with bond angles of 120° are shown in Fig. 2 and 3. Imposing periodicity on a linear chain implies that atoms are disposed on the surface of a cylinder (structure II shown in Fig. 2). The cylindrical geometry can easily be implemented within the above DMRG scheme. The annulene D_{3h} geometry, proper of $6(2n+1)$ systems¹⁷ (structure III shown in Fig. 3), requires a slight modification of the DMRG superblock arrangement, which must be changed to AB due to the lower symmetry (translation invariance is lost). We note that the sigma part of the PPP hamiltonian does not depend on bond angles. Therefore the energy difference between the various geometries is purely due to the distance difference between second and further neighbours in the molecule.

IV. ACCURACY TEST

There are two ways of improving the accuracy of a DMRG calculation: increasing the number m of states kept to describe A and performing one or more iterations of the finite-size algorithm. For comparison, we compute two sets of values, obtained respectively with the finite-size algorithm and $m = 256$ states (DMRG (1)) and with the finite-size algorithm and $m = 512$ states in the last iteration (DMRG (2)). Even when we limit ourselves to the finite-size algorithm we must use from the very beginning the hamiltonian coefficients that describe the final system, because the distances depend on the final size.

We test both methods against FCI calculations for $N = 14$. As Table I shows, the absolute error of DMRG (1) is of order $1 \cdot 10^{-2}$ eV, while the absolute error for DMRG (2) is of order $2 \cdot 10^{-4}$ eV.

TABLE I. Energy results for $N = 14$: the energies calculated with DMRG are compared to FCI values. In DMRG (1) we use the finite-size algorithm and keep 256 states. In DMRG (2) we use the finite-size algorithm and keep 512 states in the third (last) iteration. R_0 and ϵ are in A , energies in eV.

R_0	ϵ	E [DMRG (1)]	E [DMRG (2)]	E [FCI]
1.390	0.0000	-35.678793	-35.685545	-35.685710
	0.0100	-35.718946	-35.725648	-35.725808
	0.0200	-35.835913	-35.842554	-35.842695
	0.0300	-35.952880	-35.959726	-35.959913
1.400	0.0000	-34.873826	-34.880260	-34.880426
	0.0100	-34.913695	-34.920161	-34.920230
	0.0200	-35.029901	-35.036097	-35.036154
	0.0300	-35.146107	-35.152303	-35.152372
1.410	0.0000	-34.083595	-34.089740	-34.089900
	0.0100	-34.123179	-34.129256	-34.129409
	0.0200	-34.238365	-34.244233	-34.244367
	0.0300	-34.353551	-34.359419	-34.359553

Nonetheless, dimerization and average bond length are in substantial agreement: a polynomial fit of the data (even in ϵ) gives $R_0 = 1.40414A$ for DMRG (1), $R_0 = 1.40410A$ for DMRG (2) and FCI, and ϵ vanishing in all three cases. Anyway we do not learn much from the $N = 14$ case since the difficult task is the determination of ϵ . We note that the total energy is not very sensitive with respect to variations of ϵ .

For $N = 16$, ϵ is non-vanishing. In this case we test the accuracy of the method by comparing energies obtained exchanging double and single bonds. The hamiltonian with (anti)periodic boundary conditions is invariant with respect to the exchange of double and single bonds. Our arrangement used in DMRG is not invariant: the bonds connecting the blocks are always asymmetric with respect to exchange of single and double bonds and also the bonds internal to blocks A and B are asymmetric for certain numbers of sites. So the symmetry will only be recovered if convergence is accurately achieved. Let $E(+)$ ($E(-)$) denote the energy obtained with $R_{0,1}$ a double (single) bond. Table II shows these sets of energies for the case $N = 16$.

We find that DMRG (1) does not provide a very accurate determination of ϵ : minimizing over the set of energies $E(+)$ we obtain the values $R_0 = 1.40593A$, $\epsilon = 0.0236A$, while minimizing over the set of energies $E(-)$ we get a quite different minimum $R_0 = 1.40599A$, $\epsilon = 0.0240A$. DMRG (2) improves the result considerably: from the set of energies $E(+)$ we get $R_0 = 1.40577A$, $\epsilon = 0.0227(6)A$, from $E(-)$ we get $R_0 = 1.40577A$, $\epsilon = 0.0227(2)A$. Thus we see that the finite-size algorithm proves to be very useful. In order to spare computing time in this case, it is worth implementing a transformation of the wavefunction that gives a guess for starting the next iteration, as suggested by White²⁵.

TABLE II. Energy results for $N = 16$: comparison of DMRG (1) and DMRG (2) energies $E(+)$ ($E(-)$) obtained by choosing $R_{0,1}$ a double (single) bond respectively. $E(+)$ and $E(-)$ are very close for the case DMRG (2). R_0 and ϵ are in A , energies in eV.

R_0	ϵ	DMRG (1)		DMRG (2)	
		$E(-)$	$E(+)$	$E(-)$	$E(+)$
1.400	0.020	-39.908840	-39.908750	-39.920105	-39.920102
	0.025	-40.014971	-40.014343	-40.024754	-40.024635
	0.030	-40.138842	-40.138400	-40.147548	-40.147519
1.405	0.020	-39.456517	-39.456962	-39.467522	-39.467413
	0.025	-39.562115	-39.561796	-39.571654	-39.571722
	0.030	-39.685307	-39.685028	-39.693748	-39.693736
1.410	0.020	-39.008484	-39.008540	-39.019108	-39.019058
	0.025	-39.113436	-39.112946	-39.122670	-39.122689
	0.030	-39.235946	-39.235557	-39.244184	-39.244095

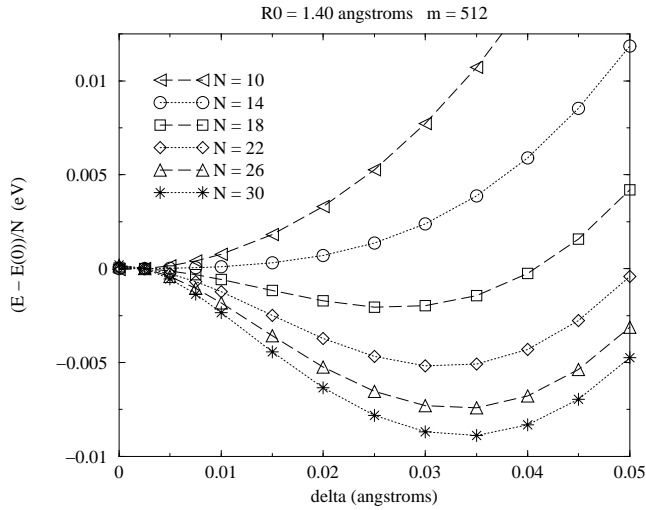


FIG. 4. Total energies at fixed $R_0 = 1.4\text{\AA}$. Results are obtained with DMRG (2). $\frac{\partial E}{\partial \delta} \Big|_{\delta=0}$ vanishes for $N = 14$.

V. RESULTS AND DISCUSSION

In Fig. 4 we show the behaviour of the energy versus fixed $R_0 = 1.40\text{\AA}$, using DMRG (2). In contrast with the case of open boundary conditions used in Ref. [18], we find $\frac{\partial E}{\partial \delta} \Big|_{\delta=0} = 0$, as expected. We observe the transition from a non-dimerized minimum for $N = 14$ to a dimerized minimum for $N = 18$.

We perform two-dimensional minimization (energy versus δ and R_0) with both DMRG (1) and DMRG (2) as shown in Fig. 5, and 6. We find a discontinuity in the slope of the curve of R_0 versus N in correspondence of the transition from a non-dimerized minimum to a dimerized one ($N > 14$).

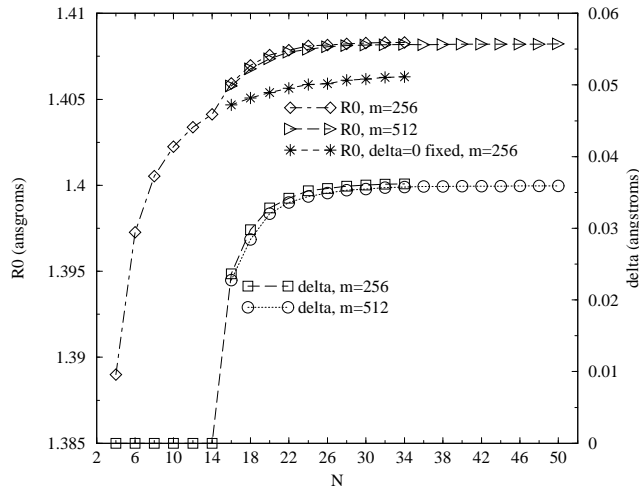


FIG. 5. Average bond length and dimerization, as determined from minimization of total energies with DMRG (1) ($m = 256$ states) and DMRG (2) ($m = 512$ states). Data denoted with a star indicate values of the average bond length obtained from minimization with the constraint $\delta = 0$.

In fact it can be seen from Fig. 5 that the curve of R_0 values obtained fixing $\delta = 0$ shows no discontinuity. The asymptotic values for R_0 and δ are approximately given by $1.408(3)\text{\AA}$ and $0.036(0)\text{\AA}$. The critical value $N = 14$ was also found by Palius and coworkers in his VB calculation¹⁶ as well as in the previous studies of the series on dimerization of PPP cyclic polyenes¹⁵. The hamiltonian used has the same two-body part, but we use a different prescription for the dependence of the hopping integral and the sigma energy $E(R_{ij})$ upon the interatomic distance. Recent DFT calculations¹⁷ on the annulenes $C_N H_N$, with $N \leq 66$ give a critical value $N = 30$, confirming and extending previous results of MP2²⁶ and DFT calculations²⁷. A direct comparison of the results is rather problematic due to the difference between the models. In our case we have a simplified hamiltonian treated at a high level of approximation by the DMRG method. On the other hand, the DFT calculation relies upon a more realistic all-electron ab-initio hamiltonian, with a poorer treatment of the long ranged electron correlations.

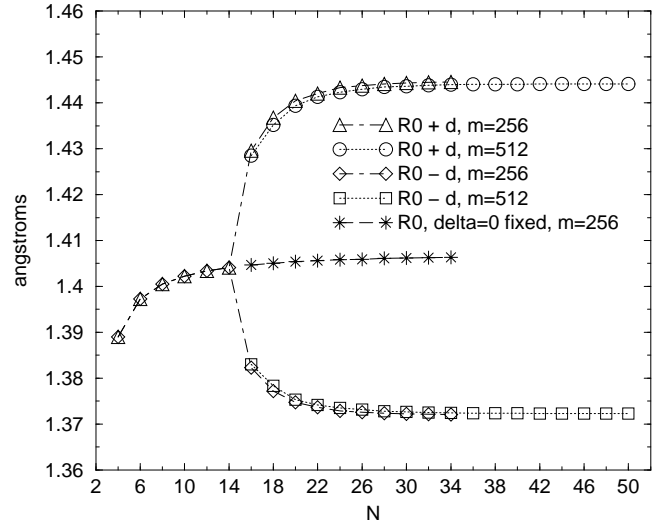


FIG. 6. Single and double bond lengths as obtained from energy minimization with both DMRG (1) and DMRG (2).

The location of the minimum of the energy as a function of R_0 and δ is the result of a balance of the E and E' energies, as can be seen from Fig. 7, and one might wonder whether a small variation of one of the two opposite terms could significantly change the results. The transition from the non alternating to the dimerized regime can be followed by considering the second derivative of the total energy (per carbon atom) with respect to δ , $E''(\delta) = E''(\delta) + E''(\delta)$. In the non alternating situation we have a minimum at $\delta = 0$, i.e. $E''(0) > 0$, while in the dimerized one we have two symmetrical minima at $\delta \neq 0$, i.e. $\delta = 0$ is now a local maximum and $E''(0) < 0$. Therefore we can study the sign of the second derivative of the energy per carbon atom as a function of the number of atoms N : at the transition point E''

must be vanishing. In Table III we report the values of E'' per carbon atom for $N = 10; 14; \dots; 30$ together with E'' per carbon atom (independent from N); it is easily seen that the transition occurs between $N = 14$ and $N = 18$. From these data it can be estimated that in order to have the transition at $N = 30$, we need to alter the ratio $E'' = E''$ by a factor 2, which cannot be considered a small adjustment of the model.

In order to check the influence of geometry on these results, we choose the special case $N = 18$, and we compare energies obtained with the three different geometries of Fig. 1-3. The energies are shown in Table IV. The geometry does not affect the dimerization in a sensible way, although the value of δ is slightly reduced by going from (I) to (III). The values are the following:

- (I) ring: $R_0 = 1.4067(6) \text{ \AA}$, $\delta = 0.0290(0) \text{ \AA}$
 (II) cylinder: $R_0 = 1.4064(7) \text{ \AA}$, $\delta = 0.0276(1) \text{ \AA}$
 (III) annulene: $R_0 = 1.4063(1) \text{ \AA}$, $\delta = 0.0271(6) \text{ \AA}$

Table IV shows that the annulene geometry is variationally preferred. However, the energy is completely unaffected by these geometry changes. The small differences in the values of R_0 and δ are only due to the part of the Hamiltonian.

TABLE III. Second derivatives of E and energies per carbon atom at zero dimerization, as obtained from DMRG (2) data. E'' does not depend on N . Derivatives are in atomic units.

N	$E''(\delta = 0)$	$E''(\delta = 0)$
10	0.6082	-0.44(0)
14	\	-0.59(1)
18	\	-0.74(9)
22	\	-0.91(1)
26	\	-1.06(7)
30	\	-1.21(2)

TABLE IV. Energy results for $N = 18$: comparison of energies from DMRG (2) with different geometries, shown in Fig. 1, 2 and 3. R_0 and δ are in \AA , energies in eV.

R_0	δ	ring (I)	cylinder (II)	annulene (III)
1.400	0.020	-44.826681	-44.913191	-44.951474
	0.025	-44.952568	-45.037015	-45.074791
	0.030	-45.098006	-45.180696	-45.217941
1.405	0.020	-44.318921	-44.404909	-44.442656
	0.025	-44.444324	-44.528098	-44.565347
	0.030	-44.589043	-44.670964	-44.707697
1.410	0.020	-43.815950	-43.901321	-43.938530
	0.025	-43.940718	-44.023869	-44.060595
	0.030	-44.084491	-44.165918	-44.202143

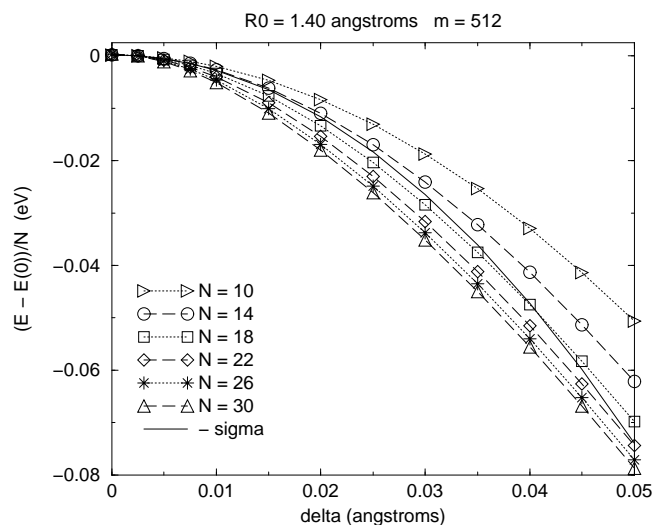


FIG. 7. Comparison of energies versus δ at fixed $R_0 = 1.4 \text{ \AA}$. The symbols denote energies per carbon atom for N between 10 and 30, the solid line denotes the opposite of the energy per carbon atom. Results are obtained with DMRG (2).

- S. R. White, Phys. Rev. Lett. 69, 2863 (1992).
- S. R. White, Phys. Rev. B 48, 10345 (1993).
- G. Fano, F. Ortolani and L. Ziosi, J. Chem. Phys. 108, 9246 (1998).
- S. R. White and D. H. Huse, Phys. Rev. B 48, 3844 (1993).
- C. Zhang, E. Jeckelmann and S. R. White, Phys. Rev. Lett. 80 2661 (1998); E. Jeckelmann and S. R. White, Phys. Rev. B 57 6376 (1998).
- L. G. Caron and S. Moukouri, Phys. Rev. B 56 R8471 (1997).
- S. R. White and D. J. Scalapino, Phys. Rev. Lett. 80 1272 (1998).
- R. G. Parr, The Quantum Theory of Molecular Electronic Structure, Benjamin, New York, 1958.
- D. Yaron et al., J. Chem. Phys. 108, 7451 (1998).
- S. Ramasesha, S. K. Pati, H. R. Krishnamurti, Z. Shuai and L. Bredas, Phys. Rev. B 54, 7598 (1996); Z. Shuai, S. K. Pati, W. P. Su, J. L. Bredas and S. Ramasesha Phys. Rev. B 55 15368 (1997).
- G. L. Bendazzoli and S. Evangelisti, Chem. Phys. Lett. 185, 125 (1991).
- G. L. Bendazzoli, S. Evangelisti and L. Gagliardi, Int. J. Quantum Chem. 51, 13 (1994).
- J. C. W. Chien, "Polyacetylene", Academic Press, Orlando San Diego San Francisco New York London Toronto Montreal Sydney Tokyo Sao Paulo, 1984 and references therein.
- Z. G. Soos and G. W. Hayden in "Electroresponsive Molecular and Polymeric Systems" edited by T. A. Skotheim, Marcel Dekker Inc., New York and Basel, 1988, p. 197.
- J. Pakdus and E. Chin, Internat. J. Quantum Chem.

- XXIV, 373 (1983); J. Pakus, E. Chin and M. G. Grey, *Internat. J. Quantum Chem.* XXIV, 395 (1983); R. Pauncz and J. Pakus, *Internat. J. Quantum Chem.* XXIV, 411 (1983).
- ¹⁶ X. Li and J. Pakus, *Internat. J. Quantum Chem.* 60, 513 (1996).
- ¹⁷ C. H. Choi and M. Kertesz, *J. Chem. Phys.* 108, 6681 (1998).
- ¹⁸ M. B. Lepetit and G. M. Pastor, *Phys. Rev. B* 56, 4447 (1997).
- ¹⁹ J. Malek, S. L. Drechsler, G. Paash, *Phys. Rev. B* 56, R8467 (1997).
- ²⁰ E. Jeckelmann, *Phys. Rev. B* 57, 11838 (1998).
- ²¹ M. Roman and R. J. Bursill, *Phys. Rev. B* 57, 15167 (1998).
- ²² M. Said, D. M. Aynau, J. P. Malrieu and M. A. Garcia-Bach, *J. Am. Chem. Soc.* 106, 571 (1994).
- ²³ N. Mataga and K. Nishimoto, *Z. Physik Chem.* 13, 140 (1957).
- ²⁴ G. L. Bendazzoli and S. Evangelisti, *Int. J. Quantum Chem.* 55, 347 (1995).
- ²⁵ S. R. White, *Phys. Rev. Lett.* 77, 3633 (1996).
- ²⁶ H. Jiao and P. v. R. Schleyer, *Angew. Chem. Int. Ed. Engl.* 35, 2383 (1996); K. K. Baldrige and J. S. Siegel, *ibidem* 36, 745 (1997).
- ²⁷ C. H. Choi, M. Kertesz and A. Karpfen, *J. Am. Chem. Soc.* 119, 11994 (1997).
- ²⁸ E. B. Starikov, *Internat. J. Quantum Chem.* 68, 421 (1998).